

# SELF-ACTIVATION PROCESS TO FABRICATE ACTIVATED CARBON FROM KENAF

*Changlei Xia*<sup>†</sup>

PhD Candidate  
E-mail: Changlei.Xia@unt.edu

*Sheldon Q. Shi*<sup>\*†</sup>

Associate Professor  
Department of Mechanical and Energy Engineering  
University of North Texas  
Denton, TX  
E-mail: Sheldon.Shi@unt.edu

(Received August 2015)

**Abstract.** Self-activation takes advantage of the gases emitted from the pyrolysis process of biomass to activate the converted carbon. Therefore, a high-performance activated carbon is obtained with no addition of activating agents. In this study, kenaf fiber was self-activated into activated carbon. The Brunauer–Emmett–Teller (BET) specific surface area ( $SA_{BET}$ ) of nonactivation and self-activation pyrolyzed at 1100°C for 2 h was analyzed and obtained as 252 and 1280 m<sup>2</sup>/g, respectively, with 408% difference. The results showed that the highest  $SA_{BET}$  (1742 m<sup>2</sup>/g) was achieved when a kenaf fiber was pyrolyzed at 1100°C for 10 h. A linear relationship was shown between the  $\ln(SA_{BET})$  and the yield of kenaf fiber–based activated carbon through the self-activation process. The study also showed that the produced activated carbon with a 9.0% yield gave the highest surface area per gram kenaf fiber (80 m<sup>2</sup>/g kenaf fiber) and those with the yields between 7.2 and 13.8% produced 95% of the greatest surface area per gram kenaf fiber (76 m<sup>2</sup>/g kenaf fiber).

**Keywords:** Self-activation, activated carbon, biomass, kenaf fibers, surface area, pyrolysis.

## INTRODUCTION

Activated carbon is a crude form of graphite with a random or amorphous structure. It is highly porous with a large internal surface area (Hamerlinck et al 1994). Activated carbon exhibits a broad range of pore sizes from visible cracks or crevices to slits of molecular dimensions. Generally, activated carbon has a specific surface area of greater than 500 m<sup>2</sup>/g as determined by the gas adsorption technique. In the adsorption analysis, nonpolar gases, eg N<sub>2</sub>, CO<sub>2</sub>, Ar, and CH<sub>4</sub>, are usually used. N<sub>2</sub> adsorption at 77 K is widely used (Mohan and Pittman 2006).

The use of carbon can be traced back to ancient times. The earliest known use of carbon in the form of wood chars (charcoal) was in 3750 BC by the Egyptians and Sumerians (Inglezakis and

Poulopoulos 2006). Activated carbon was first produced on an industrial scale in the early part of the 20th century in Europe. In the early stage, activated carbon was in the form of powder, called powdered activated carbon (PAC). Recently, many types of activated carbon, eg granular activated carbon and pelletized activated carbon, have been developed. The Swedish chemist von Ostrejko obtained two patents, in 1900 and 1901, covering the basic concepts of chemical and physical–thermal activation of carbon, with metal chlorides and with carbon dioxide and steam, respectively (Sontheimer et al 1988). In 1909, a plant named Chemische Werke was built to manufacture, for the first time on a commercial scale, the PAC Eponit from wood, adopting von Ostrejko’s gasification approach (Dabrowski 1999). Mozammel et al (2002) reported that activated carbon sales in the world market were estimated at 375,000 tons in 1990, excluding the sales in eastern Europe and China. If eastern Europe and China were considered,

\* Corresponding author

† SWST member

total sales could be more than 450,000 tons. By the late 1990s, the world market was estimated at about 700,000 tons/yr, with a market growth of about 4–6%/yr. The global activated carbon market was about \$1.8 billion in 2011 and is estimated to reach \$3.0 billion by 2016. According to a recent report, the worldwide activated carbon demand is expected to increase more than 10% per year to 1.9 Mt by 2016 (The Freedonia Group 2012).

Currently, the methods of activation include physical–thermal and chemical activation (Wikipedia 2015). Physical–thermal activation uses a mild oxidizing gas, eg CO<sub>2</sub> and water steam, to eliminate the bulk of volatile matter, followed by partial gasification during pyrolysis (Rodriguezreinoso et al 1995; Zhang et al 2004; Hameed and El-Khaiary 2008). Greater porosity and surface area can be obtained from the physical–thermal activation method. In chemical activation, chemicals are used to increase the surface area (Lua and Yang 2004; Aber et al 2009; Xu et al 2010; Zhang et al 2010; Shi et al 2015). Prior to activation, raw materials are impregnated with certain chemicals (ZnCl<sub>2</sub>, KOH, NaOH, K<sub>2</sub>HPO<sub>4</sub>, etc) and then are processed by the activation steps.

The self-activation process of biomass described in this study takes advantage of the gases emitted from the biomass during the carbonization process to serve as the activation agent. Therefore, the carbonization and activation are combined into one step (Shi and Xia 2014; Xia and Shi 2016). The literatures show that the pyrolysis gases from the biomass mainly contain H<sub>2</sub>, CO, H<sub>2</sub>O, CO<sub>2</sub>, and CH<sub>4</sub> (Yang et al 2007; Crombie and Masek 2014; Mukarakate et al 2014). Among them, CO<sub>2</sub> and H<sub>2</sub>O have been widely used as activating agents in the activated carbon manufacturing (Zhang et al 2004; Mohan and Pittman 2006). Thus, the pyrolysis gases, CO<sub>2</sub> and H<sub>2</sub>O, may serve as activating agents to activate the carbon. In our recent research, the activated carbon fabricated through the self-activation process using a kenaf core presented great specific surface area (up to 2432 m<sup>2</sup>/g) (Xia and Shi 2016). In this study, kenaf fiber was used for the self-activation process, and

the greatest specific surface area obtained was 1742 m<sup>2</sup>/g, which is comparable with that manufactured using the conventional activation processes (up to 1926 m<sup>2</sup>/g for physical activation and 1642 m<sup>2</sup>/g for chemical activation) (Yahya et al 2015). Compared with conventional activated carbon manufacturing, using self-activation saves the cost of activating agents and decreases the environmental impact, compared with conventional activation processes. Physical activation using CO<sub>2</sub> and chemical activation using ZnCl<sub>2</sub> are two common methods in the conventional activation process. Both processes introduce additional CO<sub>2</sub> (Mohan and Pittman 2006) or ZnCl<sub>2</sub> (Zhang et al 2010), from which both the CO<sub>2</sub> emission (the main emitted gas is still CO<sub>2</sub>) from the activation process and the zinc compound removal by acid from the follow-up process cause environmental concerns. However, the exhausting gases (mainly CO and H<sub>2</sub>) from the self-activation process can be used as fuel or as feedstock for methanol production with further synthesis.

In this study, the self-activation process of kenaf fiber was investigated. The parameters of self-activation, including temperature and dwelling time, were evaluated, and the effect of changes of specific surface area on the yield were elucidated. In addition, the effective use of kenaf fibers for producing the greatest total surface area is discussed.

## MATERIALS AND METHODS

### Self-activation Process

A high-temperature versatile box furnace (STY-1600C, Sentro Tech Corp., Strongsville, OH) was used for the experiment (Fig 1a). The box furnace had a type-k thermocouple with a data logger (TC101A, MadgeTech, Inc., Warner, NH) for detecting internal temperature and a digital pressure gauge (ADT680W-25-CP15-PSI-N, Additel Corp., Yorba Linda, CA) for measuring the pressure of the furnace chamber. Kenaf fiber was obtained from Ken Gro Corp., Charleston, MS. The MC of the fiber was 11.7% based on the procedure described in American Society for

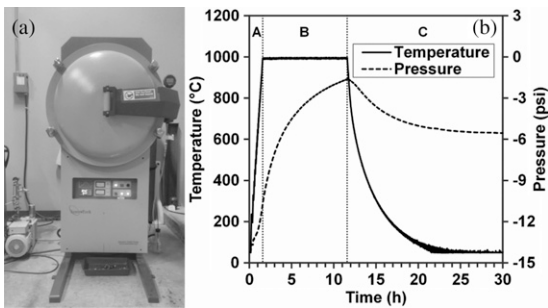


Figure 1. (a) Box furnace and (b) the internal pressure and temperature as a function of time in three pyrolysis periods: A) ramping of 10°C/min; B) dwelling for 10 h; and C) controlled cooling of 10°C/min and then self-cooling to room temperature.

Testing and Materials (ASTM) D 4442 standard (ASTM 2010). A self-activation process was conducted on the kenaf fiber. The following procedures were carried out:

1. The kenaf fiber was placed into the box furnace chamber.
2. A vacuum was applied to the furnace for about 2 h to reach a pressure of  $-97,906 \pm 34$  Pa (96.6% vacuum), and then all the values of the furnace were turned off to keep a closed system.
3. The temperature of the furnace was increased in three steps (Fig 1b): A) ramping with 10°C/min, B) dwelling, and C) cooling with no more than 10°C/min to room temperature.

### Nonactivation

A comparative experiment was designed and carried out for examining the difference between self-activation and nonactivation (Fig 2a). For the specimens with self-activation, the kenaf fiber was placed inside the furnace with no cover, which allowed the gases generated from the biomass to flow through the converted carbon material. For the specimens with nonactivation, the biomass was put in a crucible and a cap was used to cover the container, allowing limited gases to access the biomass materials. The biomass in the crucible (volume about 0.5 L) was pyrolyzed to generate gases, which flowed out of the crucible to the furnace. When the pressure reached a bal-

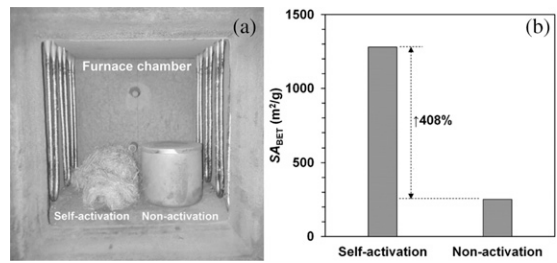


Figure 2. Self-activation vs nonactivation: (a) kenaf fibers in the furnace and (b) SA<sub>BET</sub> values.

ance inside and outside of the crucible, the gas exchange stopped. Thus, only a small amount of gases, 1.4% (0.5 L/350 L, crucible volume/furnace volume) remained in the crucible, which provided limited gas activation opportunity for the material. It was considered nonactivation.

### Characterization

Prior to characterization, the activated carbon products were crushed into a powder by an ultra-fine pulverizing machine (RT-UF26, Rong Tsong Precision Technology Co., Taichung City, Taiwan). According to ANSI/AWWA 2010, the requirements for the particle size distribution of PAC are not less than 99% of the activated carbon shall pass a no. 100 sieve, not less than 95% shall pass a no. 200 sieve, and not less than 90% shall pass a no. 325 sieve. The activated carbon sample was labeled as PAC (pyrolysis temperature, dwelling time), eg PAC (1000°C, 10 h).

The N<sub>2</sub> gas adsorption capabilities of PAC were determined by nitrogen adsorption at 77 K with a surface area and pore size analyzer (3Flex 3500, Micromeritics Instrument Corp., Norcross, GA). The samples were vacuum degassed at 350°C for 3-5 da using a degasser (VacPrep 061, Micromeritics Instrument Corp.) and then in situ degassed at 350°C for 20 h by a turbo molecular drag pump (EXT75DX 63CF, Edwards Limited, Crawley, West Sussex, UK). Specific surface areas were calculated from the isothermal plots through the instrumental software (3Flex Version 1.02, Micromeritics Instrument Corp.). The Brunauer–Emmett–Teller (BET) method was used for the specific surface area analysis. Pyrolysis

Table 1. Data summary of the pyrolysis products with different parameters.

Sample	Pyrolysis temperature (°C)	Dwelling time (h)	Yield (%)	SA <sub>BET</sub> (m <sup>2</sup> /g)
PAC (700°C, 10 h)	700	10	17.08	122
PAC (750°C, 10 h)	750	10	16.58	139
PAC (800°C, 10 h)	800	10	15.99	194
PAC (850°C, 10 h)	850	10	15.45	290
PAC (900°C, 10 h)	900	10	13.14	542
PAC (950°C, 10 h)	950	10	8.49	844
PAC (1000°C, 2 h)	1000	2	11.28	681
PAC (1000°C, 4 h)	1000	4	8.96	956
PAC (1000°C, 6 h)	1000	6	7.49	1072
PAC (1000°C, 8 h)	1000	8	6.65	1336
PAC (1000°C, 10 h)	1000	10	3.52	1534
PAC (1000°C, 15 h)	1000	15	3.20	1616
PAC (1000°C, 30 h)	1000	30	2.91	1540
PAC (1000°C, 40 h)	1000	40	2.06	1558
PAC (1000°C, 60 h)	1000	60	1.34	282
PAC (1050°C, 10 h)	1050	10	2.16	1561
PAC (1100°C, 10 h)	1100	10	2.21	1742
PAC (1150°C, 10 h)	1150	10	4.58	1460
Ash <sup>a</sup>	650	12	1.16	34

<sup>a</sup> Ash content was determined in accordance with ASTM D 2866 standard (ASTM 2011) that kenaf core was pyrolyzed in an air-atmosphere muffle furnace at 650°C for 12 h.

parameters, yields, and BET specific surface area (SA<sub>BET</sub>) are summarized in Table 1.

## RESULTS AND DISCUSSION

### Self-activation vs Nonactivation

Self-activation and nonactivation were compared by a comparative experiment (Fig 2a). Both self-activation and nonactivation were carried out at 1100°C for 2 h. The SA<sub>BET</sub> of self-activation and nonactivation were obtained as 1280 and 252 m<sup>2</sup>/g, respectively, from which a 408% increase was calculated with the self-activation compared with the nonactivation (Fig 2b). It was indicated that the converted carbon was activated by the emitted gases during the self-activation process.

### Yield vs Pyrolysis Parameters

The effect of different pyrolysis parameters (pyrolysis temperature and dwelling time) on the efficiency of the self-activation process was studied. Pyrolysis experiments were conducted on the kenaf fiber at different temperatures between

700°C and 1150°C with an interval of 50°C, dwelling for 10 h. The relationship between yield and pyrolysis temperatures is shown in Fig 3a. Four phases can be identified in Fig 3a: A) 700-880°C, B) 880-1000°C, C) 1000-1080°C, and D) 1080-1150°C. High yields (17.08-15.45%) were obtained in Phase A, compared with Phase B-D. As the pyrolysis temperature increased, the yield decreased and a slow self-activation was presented in Phase A. In Phase B, as the temperature increased from 880 to 1000°C, the yield continued to decrease and the decrease in yield accelerated (0.096%/°C) compared with that in Phase A (0.011%/°C). In Phase C, the yield reduction rate decreased to 0.027%/°C, indicating that the temperature had less effect on the yield decrease. In Phase D, yields increased as pyrolysis temperature increased. The reason could be that the decomposition rate (gases into carbon) exceeded the gasification rate of the carbon by the activating gases during Phase D (Xia and Shi 2016).

Figure 3b shows a relationship between yield and dwelling time at a pyrolysis temperature of 1000°C. As illustrated in Fig 3b, as dwelling time increased, yield decreased rapidly at the initial

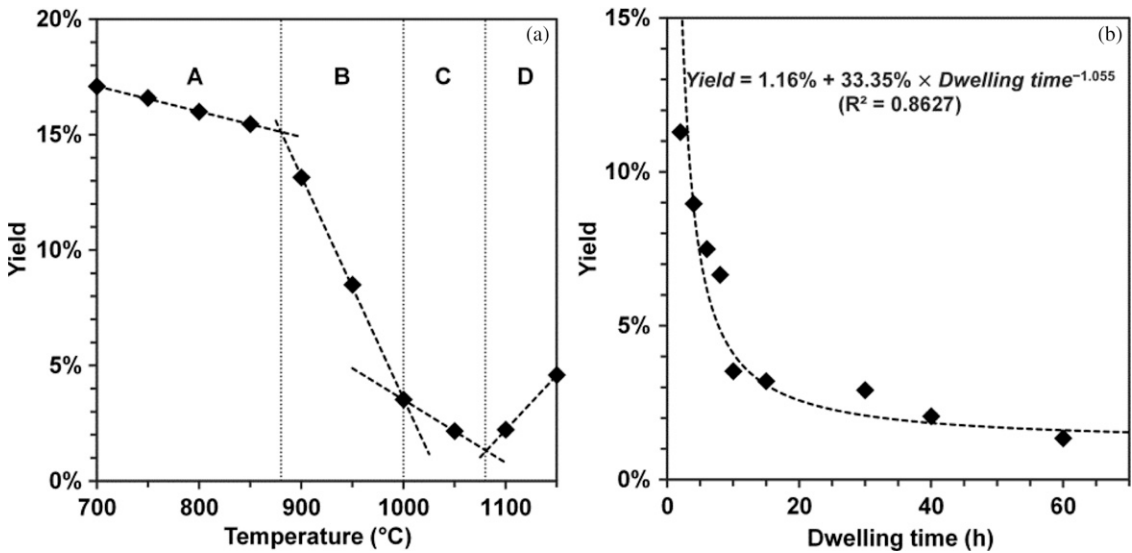


Figure 3. Yield of the activated carbon as a function of (a) pyrolysis temperature (pyrolysis time: 10 h) and (b) pyrolysis time (pyrolysis temperature: 1000°C).

stage and then slowed down until it levelled off. The process followed this exponential function:

$$Yield = 1.16\% + 33.35\% \times dwelling\ time^{-1.055} \quad (1)$$

where 1.16% is the ash content determined based on the procedure described in ASTM D 2866 standard (ASTM 2011). The coefficient of determination ( $R^2$ ) for Eq 1 was 0.8627.

### Specific Surface Area vs Pyrolysis Parameters

The effects of pyrolysis temperature and dwelling time on the  $SA_{BET}$  of activated carbon were investigated, and the results are shown in Fig 4. Changes in  $SA_{BET}$  as a function of pyrolysis temperature (dwelling time: 10 h) are shown in Fig 4a. In general,  $SA_{BET}$  increased as pyrolysis temperature increased from 700 to 1000°C and then levelled off. Figure 4b shows that  $SA_{BET}$  increased during the first 10 h and then levelled off. This phenomenon was consistent with our previous research on the self-activation for kenaf core (Xia and Shi 2016), in which  $SA_{BET}$  of produced activated carbon became constant after 15 h of self-activation (pyrolysis temperature: 1000°C). However,  $SA_{BET}$  suddenly dropped

when pyrolysis time increased from 40 to 60 h, i.e.  $SA_{BET}$  decreased from 1558 to 282  $m^2/g$ . The reason could be that the yield of the sample with 60-h pyrolysis time was 1.34%, which was very close to the ash content, 1.16%, at which  $SA_{BET}$  was only 34  $m^2/g$ .

### Yield-dependent Specific Surface Area

According to the data in Table 1, the surface area of the produced activated carbon from the self-activation process could be designed by controlling the yields. A relationship between  $\ln(SA_{BET})$  and yield (Fig 5a) was established as the following equation ( $R^2 = 0.9577$ ):

$$\ln(SA_{BET}) = -9.8460 \times yield + 7.6702 \quad (2)$$

PAC (700-850°C, 10 h) was excluded in the analysis because they had relatively lower  $SA_{BET}$  and greater yields. One possible reason could be that some volatile matter remained during the relatively low temperature (700-850°C), resulting in the blocking of pores (Xia and Shi 2016). The yield of PAC (1000°C, 60 h) was 1.34%, very close to the ash content (1.16%), causing a dramatic decrease of  $SA_{BET}$ . In general,  $SA_{BET}$  of the activated carbon increased as yield

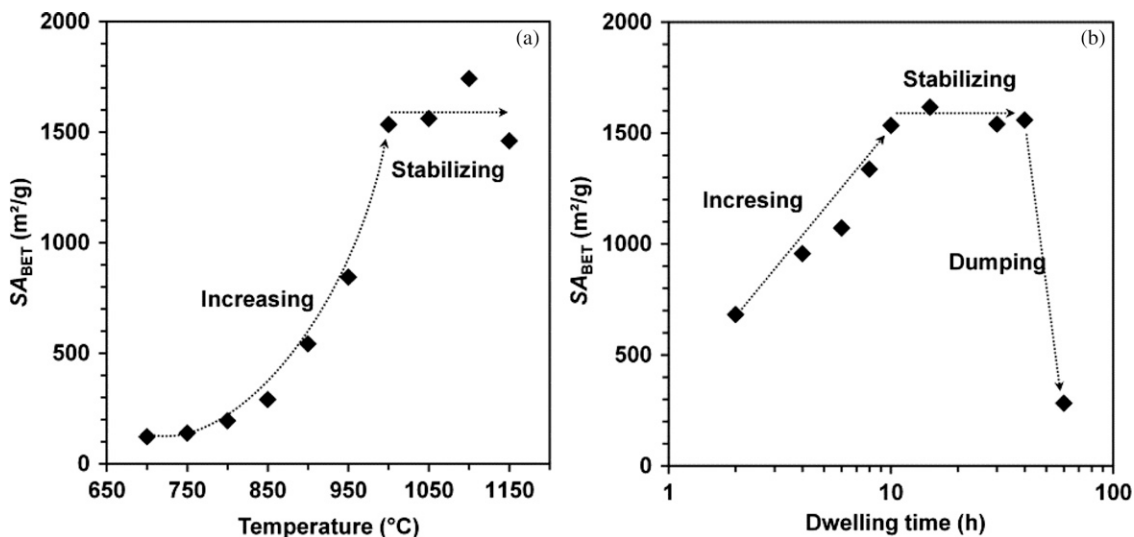


Figure 4. Specific surface area of activated carbon as a function of (a) pyrolysis temperature (pyrolysis time: 10 h) and (b) pyrolysis time (pyrolysis temperature: 1000 $^{\circ}C$ ).

decreased to a certain point and then  $SA_{BET}$  decreased until the activated carbon turned into ash. An activation model (Xia and Shi 2016) was developed to explain the effect of changes of  $SA_{BET}$  on yield. Two steps were included in the activation model, pore expansion and pore com-

bination. At the initial stage, pore expansion dominated. The small pores expanded, whereas specific surface area increased. After a certain point, pore expansion dominated. Two or more pores were combined into one pore, whereas specific surface area dramatically decreased because

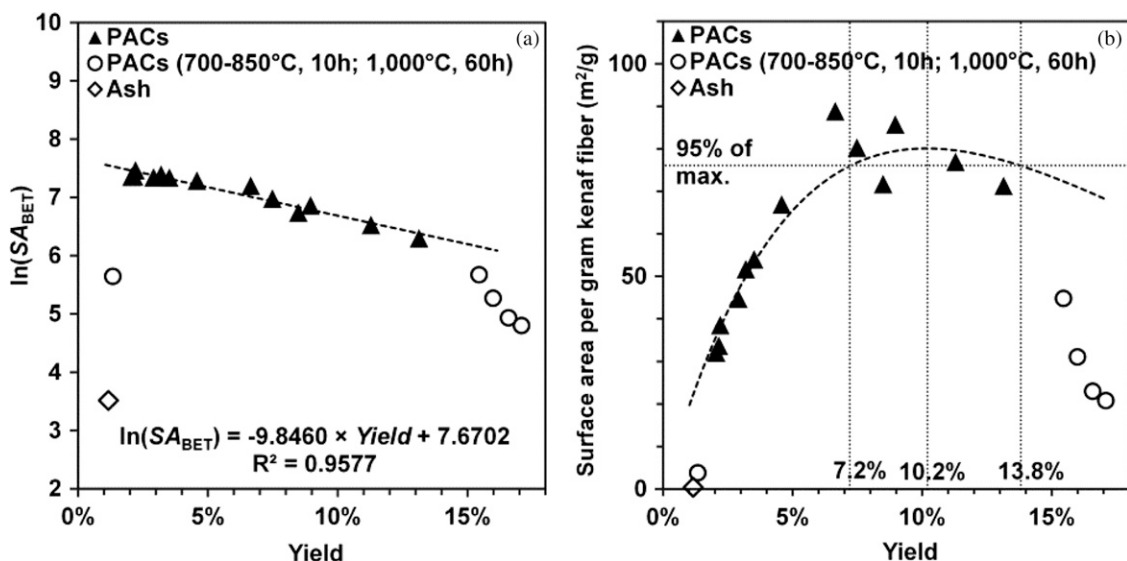


Figure 5. Relationships between yields of activated carbon and (a)  $\ln(SA_{BET})$  and (b) the total surface area produced by 1 g biomass.

of the disappearing wall between the pores. During the final stage, the produced activated carbon turned into ash.

The efficiency of total surface area generation from kenaf fiber was analyzed (Fig 5b). The surface area per gram kenaf fiber was calculated using the following equation:

$$\begin{aligned} &\text{Surface area per gram biomass} \\ &= SA_{\text{BET}} \times \text{yield} \end{aligned} \quad (3)$$

According to Eqs 2 and 3, a relationship between surface area per gram biomass and yield was established and shown in Eq 4:

$$\begin{aligned} &\text{Surface area per gram biomass} \\ &= e^{-9.8460 \times \text{yield} + 7.6702} \times \text{yield} \end{aligned} \quad (4)$$

Data calculated from Eq 4 were plotted, and as shown in Fig 5b (dashed line), the PAC with a yield of 10.2% gave the greatest surface area per gram kenaf fiber (80 m<sup>2</sup>/g biomass). Yields between 7.2% and 13.8% produced a surface area per gram kenaf fiber within 95% of the maximum (76 m<sup>2</sup>/g kenaf fiber). These results provide a guide for taking full advantage of kenaf fiber to create the maximum surface area by controlling the yields.

### CONCLUSIONS

Self-activation is an effective activation process for activated carbon from biomass. Kenaf fiber-based activated carbon was successfully produced using the self-activation process without introducing additional activating gases or chemicals. Comparisons of self-activation and nonactivation showed that surface area of produced carbon can be dramatically increased. The relationships between yields and surface area ( $SA_{\text{BET}}$ ) were found to have a lineal fitting between  $\ln(SA_{\text{BET}})$  and yields. In addition, the study of kenaf fiber's effectiveness for producing greatest total surface area showed that a yield of 10.2% received a maximum surface area per gram kenaf fiber, and yields between 7.2% and 13.8% were recommended to obtain an effectiveness of more than 95% of the maximum.

### ACKNOWLEDGMENTS

We thank Liping Cai (Mechanical and Energy Engineering, University of North Texas) for help with this project and Angela Nelson (College of Engineering, University of North Texas) for proof reading.

### REFERENCES

- Aber S, Khataee A, Sheydaei M (2009) Optimization of activated carbon fiber preparation from kenaf using K<sub>2</sub>HPO<sub>4</sub> as chemical activator for adsorption of phenolic compounds. *Biores Technol* 100(24):6586-6591.
- ANSI/AWWA (2010) ANSI/AWWA B600 Powdered activated carbon. American National Standards Institute/American Water Works Association, Denver, CO. <http://dx.doi.org/10.12999/AWWA.B600.10> (11 January 2016).
- ASTM (2010) D 4442. Standard test methods for direct moisture content measurements of wood and wood-base materials. American Society for Testing and Materials, West Conshohocken, PA. <http://www.astm.org/Standards/D4442.htm> (11 January 2016).
- ASTM (2011) D 2866. Standard test method for total ash content of activated carbon. American Society for Testing and Materials, West Conshohocken, PA. <http://www.astm.org/Standards/D2866.htm> (11 January 2016).
- Crombie K, Masek O (2014) Investigating the potential for a self-sustaining slow pyrolysis system under varying operating conditions. *Biores Technol* 162:148-156.
- Dabrowski A (1999) Adsorption—its development and application for practical purposes. *Stud Surf Sci Catal* 123:3-68. <http://www.sciencedirect.com/science/article/pii/S0167299199805485> (11 January 2016).
- Hameed BH, El-Khaiary MI (2008) Equilibrium, kinetics and mechanism of malachite green adsorption on activated carbon prepared from bamboo by K<sub>2</sub>CO<sub>3</sub> activation and subsequent gasification with CO<sub>2</sub>. *J Hazard Mater* 157(2):344-351.
- Hamerlinck Y, Mertens D, Vansant E (1994) Activated carbon principles in separation technology. Elsevier, New York, NY.
- Inglezakis V, Pouloupoulos S (2006) Adsorption, ion exchange and catalysis: Design of operations and environmental applications. Elsevier, New York, NY. <http://www.sciencedirect.com/science/book/9780444527837> (11 January 2016).
- Lua AC, Yang T (2004) Effect of activation temperature on the textural and chemical properties of potassium hydroxide activated carbon prepared from pistachio-nut shell. *J Colloid Interface Sci* 274(2):594-601.
- Mohan D, Pittman CU Jr. (2006) Activated carbons and low cost adsorbents for remediation of tri- and hexavalent chromium from water. *J Hazard Mater* 137(2):762-811.

- Mozammel HM, Masahiro O, Bhattacharya SC (2002) Activated charcoal from coconut shell using  $ZnCl_2$  activation. *Biomass Bioenerg* 22(5):397-400.
- Mukarakate C, Watson MJ, ten Dam J, Baucharel X, Budhi S, Yung MM, Ben H, Iisa K, Baldwin RM, Nimlos MR (2014) Upgrading biomass pyrolysis vapors over  $\beta$ -zeolites: Role of silica-to-alumina ratio. *Green Chem* 16(12):4891-4905.
- Rodriguezreinoso F, Molinasabio M, Gonzalez MT (1995) The use of steam and  $CO_2$  as activating agents in the preparation of activated carbons. *Carbon* 33(1):15-23.
- Shi SQ, Che W, Liang K, Xia C, Zhang D (2015) Phase transitions of carbon-encapsulated iron oxide nanoparticles during the carbonization of cellulose at various pyrolysis temperatures. *J Anal Appl Pyrolysis* 115:1-6.
- Shi SQ, Xia C (2014) Porositization process of carbon or carbonaceous materials. US patent 14/211,357. <http://www.google.com/patents/US20140264143> (11 January 2016).
- Sontheimer H, Crittenden JC, Summers RS, Hubele C (1988) Activated carbon for water treatment. <http://hdl.handle.net/10068/237172> (11 January 2016).
- The Freedonia Group (2012) World activated carbon to 2016. <http://www.freedoniagroup.com/brochure/28xx/2878smwe.pdf> (11 January 2016).
- Wikipedia (2015) Activated carbon. [https://en.wikipedia.org/wiki/Activated\\_carbon](https://en.wikipedia.org/wiki/Activated_carbon) (11 January 2016).
- Xia C, Shi SQ (2016) Self-activation for activated carbon from biomass: Theory and parameters. *Green Chem*, doi:10.1039/C5GC02152A.
- Xu B, Chen Y, Wei G, Cao G, Zhang H, Yang Y (2010) Activated carbon with high capacitance prepared by NaOH activation for supercapacitors. *Mater Chem Phys* 124(1):504-509.
- Yahya MA, Al-Qodah Z, Ngah CWZ (2015) Agricultural bio-waste materials as potential sustainable precursors used for activated carbon production: A review. *Renew Sustain Energy Rev* 46:218-235.
- Yang H, Yan R, Chen H, Lee DH, Zheng C (2007) Characteristics of hemicellulose, cellulose and lignin pyrolysis. *Fuel* 86(12-13):1781-1788.
- Zhang TY, Walawender WP, Fan LT, Fan M, Daugaard D, Brown RC (2004) Preparation of activated carbon from forest and agricultural residues through  $CO_2$  activation. *Chem Eng J* 105(1):53-59.
- Zhang H, Yan Y, Yang L (2010) Preparation of activated carbon from sawdust by zinc chloride activation. *Adsorption* 16(3):161-166.